



Computational poroelasticity — A review

José M. Carcione¹, Christina Morency², and Juan E. Santos^{3,4}

ABSTRACT

Computational physics has become an essential research and interpretation tool in many fields. Particularly in reservoir geophysics, ultrasonic and seismic modeling in porous media is used to study the properties of rocks and to characterize the seismic response of geologic formations. We provide a review of the most common numerical methods used to solve the partial differential equations describing wave propagation in fluid-saturated rocks, i.e., finite-difference, pseudospectral, and finite-element methods, including the spectral-element technique. The modeling is based on Biot-type theories of dynamic poroelasticity, which constitute a general framework to describe the physics of wave propagation. We explain the various techniques and discuss numerical implementation aspects for application to seismic modeling and rock physics, as, for instance, the role of the Biot diffusion wave as a loss mechanism and interface waves in porous media.

INTRODUCTION

The theories of poroelasticity are essential in many geophysical applications where pore-filling materials are of interest, e.g., oil exploration, gas-hydrate detection, seismic monitoring of CO₂ storage, and hydrogeology. The most popular theory was developed by Maurice Biot in the 1950s (e.g., Biot, 1962; Bourbié et al., 1988; Allard, 1993; Carcione, 2007, pp. 235–320), who obtained the dynamic equations for wave propagation in a fully saturated medium. The theory assumes that anelastic effects arise from viscous interaction between a fluid and a solid, and it predicts two compressional waves and one shear wave. Basically, the fast P-wave has solid and fluid motions in phase, and the slow (Biot) P-wave has out-of-phase motions. At low frequencies, the slow wave becomes diffusive because the fluid-viscosity effects dominate the inertial effects. At high fre-

quencies, the inertial effects are predominant and the slow wave is activated, although under realistic conditions (low permeability, high clay content, etc.) this mode is also diffusive at high frequencies.

A major cause of attenuation in porous media is wave-induced fluid flow, which occurs at different spatial scales — macroscopic, mesoscopic, and microscopic (e.g., Pride et al., 2004). The attenuation mechanism predicted by Biot's theory takes place at macroscopic scales. It is the wavelength-scale pressure-equilibration mechanism occurring between the peaks and troughs of the P-wave. The frequency of the relaxation peak is $f_B \approx \eta \phi \rho_f / [2\pi \kappa \rho_f (\rho T - \phi \rho_f)]$ (see Table 1 for the meaning of the symbols), where $\rho = \phi \rho_f + (1 - \phi) \rho_s$ is the bulk density and the subscript B refers to Biot. The relaxation peak is generally located at the high frequencies on the order of tens of kilohertz.

At seismic frequencies, the mesoscopic loss mechanism seems to be the most important. For instance, for mesoscopic patches of gas in a water-saturated sandstone, diffusion of pore fluid in and out between different patches dissipates energy through conversion of energy to the diffusive slow mode. The patches are assumed to be much larger than the grain sizes but much smaller than the wavelength of the pulse. White (1975) was the first to introduce this loss mechanism in the framework of Biot's theory. The corresponding peak frequency is $f_M \approx \kappa K_f / (\phi \eta d^2)$, where d is the size of the patches and the subscript M refers to mesoscopic.

The microscopic mechanism is the so-called squirt flow (e.g., Pride et al., 2004), by which there is flow from fluid-filled microcracks (grain contacts) to the pore space and vice versa. This mechanism, which is not described by Biot theory, has a peak frequency $f_{SF} \approx (h/R)^2 K_f / \eta$, where h/R is the crack-thickness-to-crack-length ratio, and the mechanism is believed to be important at high frequencies. According to the values of Table 1, $f_B = 106$ kHz, $f_M = 42$ Hz, and $f_{SF} = 2.5$ MHz, where we assume $d = 20$ cm and an aspect ratio $h/R = 0.001$.

Seismic modeling is a technique for simulating wave propagation in the earth. The objective is to predict the seismogram that a set of sensors would record, given an assumed structure and composition

Manuscript received by the Editor 2 December 2009; revised manuscript received 11 February 2010; published online 14 September 2010.

¹Istituto Nazionale di Oceanografia e di Geofisica Sperimentale (OGS), Trieste, Italy. E-mail: jcarcione@inogs.it.

²Princeton University, Department of Geosciences, Princeton, New Jersey, U.S.A. E-mail: cmorency@princeton.edu.

³Universidad Nacional de La Plata, CONICET, Departamento de Geofísica Aplicada, Facultad de Ciencias Astronómicas y Geofísicas, La Plata, Argentina.

⁴Purdue University, Department of Mathematics, West Lafayette, Indiana, U.S.A. E-mail: santos@math.purdue.edu.

of the subsurface. This technique is a valuable tool for seismic interpretation and an essential part of seismic inversion algorithms. There are many approaches to seismic modeling. We classify them into three main categories of methods: direct, integral equation, and ray tracing. In this work, we focus on the first class of methods, which is the most used to solve the equations of dynamic poroelasticity. These include finite-difference (FD), pseudospectral (PS), low-order finite-element (FE), and spectral finite-element (SE) methods.

To solve the wave equation by direct methods, the geologic model is approximated by a numerical mesh; that is, the model is discretized into a finite number of points. Direct methods are also called grid methods and full-wave-equation methods, the latter because the solution provides the full wavefield. Direct methods do not have restrictions on the material variability and can be very accurate when a sufficiently fine grid is used. Furthermore, these techniques are well suited for generating snapshots, which can be an important aid in interpreting the results.

A key area of numerical modeling in poroelastic media that is worth mentioning but not discussed here is reflectivity methods. These methods have been implemented for flat layers (Stern et al., 1985; Turgut and Yamamoto, 1988) and for cylindrical structures (Rosenbaum, 1974). They are based on propagator-matrix computations in the frequency-wavenumber domain.

It is important to point out when poroelastic effects are and are not relevant. Generally, reflections at single interfaces and propagation in homogeneous media can be simulated with equivalent elastic or viscoelastic formulations (Gurevich, 1996; Carcione, 1998). In the case of interface waves and in the presence of heterogeneities at spatial scales less than the wavelength of the signal, poroelastic effects become important (e.g., mesoscopic losses). Moreover, the algorithms can be useful as research tools and in practical applications (such as patchy saturated rocks), where analytical methods are precluded.

The numerical methods discussed here consider all frequency ranges, to be applied at seismic, sonic, and laboratory frequencies. Indeed, knowledge of the input parameters to compute synthetic seismograms requires high-frequency calibration data and a proper understanding and simulation of the physics.

A detailed review of the different direct methods can be found in Carcione et al. (2002), where the authors discuss the time integration, calculation of spatial derivatives, source implementation,

physical boundary conditions, and absorbing boundaries. Here, we present the numerical aspects strictly related to the poroelastic nature of the differential equations — specifically, the methods and computational experiments.

BIOT'S EQUATIONS

In this section, a brief outline of the equations and physics involved is given. For simplicity and clarity, we consider the partial differential formulation given by Biot (1962) without the shear wave. Although this wave is important, since there are additional slow shear modes when the pore-filling material is solid (e.g., Carcione and Seriani, 2001), the poroacoustic equations are representative of the physics of porous media. By taking the solid rigidity equal to zero, we only model dilatational deformations, i.e., the P-waves.

Furthermore, for simplicity, we consider the 1D velocity-pressure formulation of Biot's theory, including the Johnson-Koplic-Dashen (JKD) dynamic permeability model (Johnson et al., 1987) to describe memory drag forces accounting for the interaction between the pore fluid and the pore walls at all frequencies. The differential equations are

$$\rho \dot{v} + \rho_f \dot{q} = -\partial_x p, \quad (1a)$$

$$\rho_f \dot{v} + m \dot{q} = -\partial_x p_f - \frac{\eta}{\kappa} \left(\frac{D}{a} + 1 \right)^{1/2} q, \quad (1b)$$

$$-\dot{p} = K_G \partial_x v + \alpha M \partial_x q + s, \quad (1c)$$

$$-\dot{p}_f = M(\partial_x q + \alpha \partial_x v) + s_f \quad (1d)$$

(Lu and Hanyga, 2004; Masson et al., 2006; Carcione, 2007), where v and q are the solid and fluid (relative to the solid) particle velocities and where p and p_f are the bulk and fluid pressures, respectively. In addition, $q = \phi(v_f - v) = \phi(\dot{u}_f - \dot{u})$, where ϕ is the effective porosity and u are the respective displacements. A dot above a variable denotes time differentiation, and ∂_x is the spatial derivative. Moreover, $K_G = K_m + \alpha^2 M$ is the Gassmann bulk modulus, with $\alpha = 1 - K_m/K_s$, $M = K_s/(1 - \phi - (K_m/K_s) + (\phi K_s/K_f))$, where K_s , K_m , and K_f are the bulk moduli of the solid, matrix, and fluid, respectively; η is the dynamic fluid viscosity; κ is the global static permeability; $\rho = (1 - \phi)\rho_s + \phi\rho_f$ is the composite density, with ρ_s and ρ_f the solid and fluid densities; and $m = T\rho_f/\phi$, with T the tortuosity, a dimensionless parameter that depends on the pore geometry. (The sandstone given in Table 1 has $K_G = 14.3$ GPa and $\rho = 2062$ kg/m³.)

Equation 1b is a generalization of Darcy's law. The differential operator $((D/a) + 1)^{1/2}$ is a shifted fractional derivative operator, where $D = \partial_t$ is the time derivative ($i\omega$ is in the frequency domain, where $i = \sqrt{-1}$ and ω is the angular frequency). It is $(D + a)^{1/2} q = \exp(-at)D^{1/2}[\exp(at)q]$, where $D^{1/2}$ represents the Caputo fractional derivative (Caputo, 1969). The parameter $a = \omega_T/K$, where $\omega_T = \eta\phi/(\rho_f T\kappa)$ is a transition frequency and $K = 4Tk/(\Lambda^2\phi)$ is a geometric factor; Λ is the pore-volume-to-grain-surface ratio (e.g., Carcione, 2007; his equation 7.242). If $\eta = 0$, the slow mode is a wave at all frequencies; otherwise, the theory predicts a diffusive-static mode at seismic frequencies.

The associated time-domain dynamic permeability $\bar{\kappa}$ to equations 1 is

Table 1. Input values for water-saturated sandstone.

Material	Parameter	Value
Grain	Bulk modulus, K_s	40 GPa
	Density, ρ_s	2500 kg/m ³
Matrix	Porosity, ϕ	0.3
	Bulk modulus, K_m	10 GPa
	Permeability, κ	200 md ^b
	Tortuosity, T	2.3
Fluid	Bulk modulus, K_f	2.5 GPa
	Density, ρ_f	1040 kg/m ³
	Viscosity, η	1 cp ^a

^a1 cp = 10⁻³ Pa

^b1 md ≈ 10⁻¹⁵ m²

$$\bar{\kappa} = \kappa \left[\left(\frac{D}{a} + 1 \right)^{1/2} + \frac{D}{\omega_T} \right]^{-1}. \quad (2)$$

The choice $D = 0$ inside the square root [$\bar{\kappa} = \kappa(1 + (D/\omega_T))^{-1}$] gives Biot's poroacoustic equations (Carcione and Quiroga-Goode, 1995), whereas the approximation $\omega \ll \omega_T$ yields $\bar{\kappa} = \kappa\{1 + [(1/2a) + (1/\omega_T)]D\}^{-1}$, i.e., the low-frequency equations obtained by Masson et al. (2006). Lu and Hanyga (2004) refer to this as the JKD model, which is quite general and matches experimental data very well. At low frequencies, the flow in the pores is laminar. At high frequencies, inertial effects dominate the shear viscous forces, resulting in relative flow except at the grain walls, where the relative motion at the viscous boundary layer is zero. The thickness of this layer decreases as $\omega^{-1/2}$ increases.

Generally, the application of the source considers three cases. The first case is a bulk source that assumes the energy is partitioned between the two phases. In this case, the relation between the solid and fluid source strengths is equal to $(1/\phi) - 1$. In the above particle-velocity/pressure formulation, this means $s = s_f$. Case two is a source in the solid; in this case, $s_f = 0$. In the third case, the source is in the fluid and $s = \phi s_f$.

FINITE-DIFFERENCE AND PSEUDOSPECTRAL METHODS

We present the developments of numerical poroelasticity in a nearly chronological order. The details about the numerical methods — FD and PS spatial differentiation and time integration — for solving the wave equation are summarized in Carcione et al. (2002) and are not discussed here (see details in Carcione 2007, pp. 385–426). For a comprehensive review of all theories and physical phenomena regarding poroelastic wave propagation, refer to Müller et al. (2010).

Early works

The first papers about the simulation of Biot waves with direct grid methods date to the 1970s. To our knowledge, Garg et al. (1974) were the first to use them. They compute 1D Green's functions (artificially damped) with an FD method. In the 1980s, Mikhailenko (1985) solved Biot's equations with no loss ($\eta = 0$) in cylindrical coordinates, with a finite Hankel transform along the radial coordinate (i.e., with constant material properties along this direction) and an FD scheme along the vertical direction, second-order accurate in space and time, i.e., $o(2,2)$. Hassanzadeh (1991) first solved Biot's low-frequency poroacoustic equations, written in the dilatation formulation ($e = \partial_x u$ and $\varepsilon = \partial_x u_f$), by using an $o(2,2)$ FD scheme. He uses the stability condition $dt < dx/(\sqrt{2}v_p)$, where dt is the time step, dx is the grid spacing, and v_p is the high-frequency-limit fast P-wave velocity. Boundary conditions at interfaces are open and explicitly satisfied (the so-called homogeneous formulation). The code is not tested against an analytical solution. The applications involve cross-well experiments, and Hassanzadeh shows that the conversion from fast P-waves to slow P-modes (diffusive) is significant.

Zhu and McMechan (1991) solve the corresponding 2D P–S-wave equations using the displacement formulation (locally homogeneous) and an $o(2,2)$ FD scheme similar to that of Hassanzadeh (1991). On the other hand, Dai et al. (1995) use an $o(2,4)$ McCormack predictor-corrector scheme, based on a dimensional (spatial) splitting technique. The stability criterion is based on the fast

P-wave, and they test the method against an analytical solution with a propagating slow wave. In Dai et al.'s work, the free surface is modeled for the first time with finite differences. The method of characteristics (e.g., Carcione et al., 2002) stabilizes the solution and sets the stress components and fluid pressure to zero. These works do not simulate and test the slow static mode.

Özdenvar and McMechan (1997) develop a PS staggered-grid algorithm for the poroelastic differential equations expressed in the displacement formulation. The time derivatives are computed with a second-order Euler forward approximation. The standard stability criterion for P-waves is used, and the numerical results are not tested with analytical solutions.

Stiffness of Biot's equations and the slow mode

Carcione and Quiroga-Goode (1995) show that the stiffness of the differential equations requires a special treatment; they were the first to model the Biot slow (static or diffusive) mode at low frequencies and to compare the simulation to an analytical solution. The low-frequency theory is given by equations 1, but the second equation becomes

$$\rho_f \dot{v} + m \dot{q} = -\partial_x p_f - \frac{\eta}{\kappa} q. \quad (3)$$

They recast the dynamic equations in the particle-velocity–pressure formulation having the matrix form $\dot{\mathbf{v}} = \mathbf{H}\mathbf{v}$, where \mathbf{v} is the field vector and \mathbf{H} is the propagation matrix.

Let us assume constant material properties and a plane-wave kernel of the form $\exp(i\mathbf{k} \cdot \mathbf{x} - i\omega_c dt)$, where \mathbf{k} is the real wavenumber vector, \mathbf{x} is the position vector, and ω_c is a complex angular frequency. Substituting the plane-wave kernel into the wave equation yields an eigenvalue equation for the eigenvalues in the $i\omega_c$ complex plane. All eigenvalues of \mathbf{H} have a negative real part. Although the eigenvalues of the fast wave have a small real part, the eigenvalues of the slow wave (in the diffusive regime) have a large real part. The presence of this diffusive mode makes Biot's differential equations stiff. The best algorithm would be an implicit method, which is unconditionally stable in the left complex plane; however, the problem resides in the accuracy to resolve the static mode. The largest negative eigenvalue corresponds to the slow mode,

$$\lambda = -\frac{\eta}{\kappa} \left(\frac{\rho}{\rho m - \rho_f^2} \right), \quad (4)$$

which should lie in the left-half $i\omega$ -plane. In other words, to be physically stable, the medium must satisfy $\rho m - \rho_f^2 > 0$; otherwise, exponentially growing modes would exist.

Carcione and Quiroga-Goode (1995) propose two time-integration methods to solve equations 1. The first is based on second-order staggered finite differences, which is A-stable, i.e., the domain of convergence is the open left-half $i\omega$ plane. The second is based on a partition or (temporal) splitting of the dynamic equations, similar to the Strang scheme. Both techniques use the PS method to compute the spatial derivatives. In the second technique, Biot's equations are partitioned into a stiff part and a nonstiff part, such that the evolution operator can be expressed as $\exp(\mathbf{H}_r + \mathbf{H}_s)t$, where r indicates the regular matrix and s is the stiff matrix. (The latter contains terms proportional to η/κ .) The product formulas $\exp(\mathbf{H}_r t)\exp(\mathbf{H}_s t)$ and $\exp((1/2)\mathbf{H}_s t)\exp(\mathbf{H}_r t)\exp((1/2)\mathbf{H}_s t)$ are first- and second-order

accurate, respectively. The stiff part is solved analytically, and the nonstiff part is solved with a fourth-order Runge-Kutta scheme.

A snapshot in poroacoustic media is displayed in Figure 1a, which shows the pressure field p resulting from a fluid source. Above the interface, $\eta = 1$ cp; below the interface, $\eta = 0$. The fast P-wave (P1) and the slow P-wave (P2) can be seen, the latter below the interface. Above the interface, the slow mode is diffusive.

Anisotropy

The 2D particle velocity–stress anisotropic equations for P- and S-waves were first solved by Carcione (1996), showing that the slow P-wave may have cusps, just as with the S-wave, and anomalous polarizations. He uses the splitting technique and proposes to approximate the time-domain dynamic permeability or JKD model with a discrete set of Zener mechanical models. The method requires additional (memory) variables as in the viscoelastic case. Although the exponential kernel associated with the generalized Zener model does not satisfy the high-frequency dependence $\omega^{-1/2}$, the approximation is appropriate for band-limited sources.

Figure 1b shows a snapshot where all of the modes are propagating waves. The particle velocity v_y in an anisotropic poroelastic homogeneous medium, where the fluid has zero viscosity, is displayed;

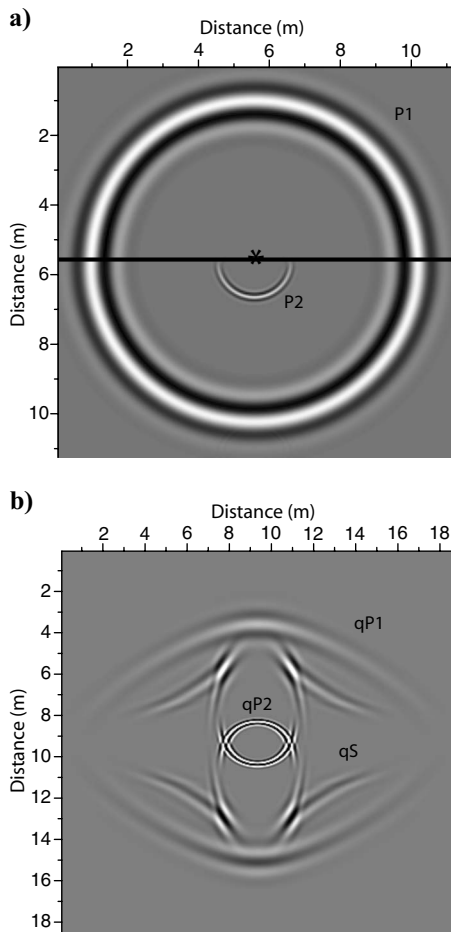


Figure 1. (a) Snapshot of the pressure field p from a fluid source applied to a poroacoustic medium, and (b) particle velocity v_y in an anisotropic poroelastic homogeneous medium, where the fluid has zero viscosity.

qP1, qS, and qP2 denote the fast quasi-P-wave, the quasi-S-wave, and the slow quasi-P-wave. The qP2-wave shows cuspidal triangles just as the shear wave does, indicating that the polarization vector has strong deviations from the normal direction to the wavefront.

Poroviscoelasticity

Carcione (1998) introduces poroviscoelasticity in numerical modeling by generalizing the fluid-solid stiffness M to a relaxation function of the Zener type in an attempt to model the squirt-flow mechanism. In addition, he obtains the effective viscoelastic differential equations by matching the Biot and squirt-flow relaxation peaks with Zener elements associated with the P and S plane-wave moduli. The solver is based on memory variables. The fit with the Zener kernels is almost perfect for realistic values of the dissipation factor. In his work, the mesoscopic loss effect is simulated for the first time considering periodic fine layers of gas and water saturating the same porous medium (matrix or skeleton) (Carcione, 1998; his Figure 7). The modeling is improved by Carcione and Helle (1999), who introduce the staggered Fourier method to compute the spatial derivatives, eliminating undesired numerical artifacts present in the regular Fourier method.

Arntsen and Carcione (2001) use this approach to fit the first observation of the slow wave in a natural sandstone at ultrasonic frequencies. Making the dry-rock shear moduli viscoelastic (i.e., time dependent), along with the coupling modulus M and the viscosity/permeability factor η/κ , is enough to predict the observed amplitudes.

Figure 2 shows a microseismogram obtained by Kelder and Smeulders (1997) for Nivelsteiner Sandstone as a function of the angle of incidence θ compared to a numerical microseismogram obtained with Biot's poroviscoelastic theory. The events are the fast compressional wave, the shear wave, the first multiple reflection of the fast compressional wave, and the slow wave. The discrepancy in the FP wave amplitude after the critical angle (approximately 32°) is because the source is closer to the sample compared to the laboratory experiments.

Nonregular mesh

A scheme based on irregular grids, allowing for surface topography and curved interfaces, has been introduced by Zhang (1999). The algorithm uses staggered quadrangle cells and solves the velocity-stress formulation. To obtain nonrectangular cells, the physical domain is mapped into square cells using the chain rule to obtain the spatial derivatives. The time integration is the typical staggered scheme, with particle velocities computed at $t + dt/2$ and stress components at $t + dt$. The Biot static mode is observed in the snapshots.

Composite porous media and Biot-type theories

Carcione and Seriani (2001) develop a numerical algorithm for simulating wave propagation in frozen porous media, where the pore space is filled with ice and water. The model, based on a Biot-type three-phase theory obtained from first principles, predicts three P-waves and two S-waves at the high-frequency limit and the corresponding diffusive modes at low frequencies. Attenuation is modeled with Zener relaxation functions, which allow a differential formulation based on memory variables. The generalization of these differential equations to the variable porosity case is given in Car-

cione et al. (2003b) by using the analogy with the two-phase case and the complementary energy theorem. A more rigorous generalization is given in Santos et al. (2004a). In this way, it is possible to simulate propagation in a frozen porous medium with fractal variations of porosity and therefore varying freezing conditions. A generalization of the splitting method to the three-phase case is performed to solve these equations.

The simulation of two slow waves from capillary forces in a partially saturated porous medium is presented in Carcione et al. (2004), based on the theory developed by Santos et al. (1990a, 1990b). The pores are filled with a wetting fluid and a nonwetting fluid, and the model, based on a Biot-type three-phase theory, predicts three P-waves and one S-wave. Again, realistic attenuation is modeled with exponential relaxation functions and memory variables. Surface-tension effects in the fluids, which are not considered in the classical Biot theory, cause the presence of a second slow wave, which is faster than the classical Biot slow wave.

An alternative theory of poroelasticity derived by Hickey and co-workers (see Quiroga-Goode et al., 2005), includes, in addition to Biot's theory, thermoelastic coupling and a differential equation describing temporal variations of porosity. Using numerical modeling based on the PS method, Quiroga-Goode et al. (2005) show that the two theories yield similar results in homogeneous media and that the additional effects are insignificant, confirming the assumptions made by Biot to establish his theory.

Mesoscopic loss mechanism and wave propagation

The mesoscopic loss mechanism was first verified by performing wave-propagation numerical experiments. Carcione et al. (2003b) use the poroelastic PS modeling algorithm to obtain the phase velocity and quality factor Q of White's model, consisting of a homogeneous sandstone saturated with brine and spherical gas pockets. The gas saturation varies by increasing the radius of the gas pocket or by increasing the density of gas bubbles. Although the modeling is two dimensional and interaction between the gas pockets is neglected in White's model, the numerical results show the trends predicted by the theory, i.e., increase in velocity at high frequencies and low permeabilities. Similar tests in more realistic (fractal) media are performed by Helle et al. (2003), showing that partial saturation is a more efficient loss mechanism than variable permeability (or porosity) and matrix heterogeneities at the mesoscopic scale. A seismic application of poroviscoelastic modeling, including the mesoscopic loss, for monitoring underground CO₂ storage can be found in Carcione et al. (2006).

Code implementation and absorbing boundaries

Code performance and elimination of artifacts from the edges of the mesh are important. A classical implementation of the 3D poroelastic equations based on an $o(2,4)$ fully staggered scheme is given by Aldridge et al. (2005), who show how to optimize the algorithm using domain decomposition methods. They find that poroelastic modeling can be two to six times more expensive than single-phase modeling. The popular perfectly matched-layer (PML) absorbing-boundary method is implemented by Zeng et al. (2001), who use an $o(2,2)$ FD scheme to solve the 3D displacement formulation of the poroelastic equations. The convolutional form of the method (C-PML) is described by Martin et al. (2008) using the classical staggered scheme.

Dynamic permeability and fractional derivatives

Lu and Hanyga (2004) and Hanyga and Lu (2005) design a numerical method to solve the time-domain particle-velocity-stress poroelastic equations, including the JKD dynamic permeability as in equations 1. The system is evolved with a predictor-corrector scheme, and the spatial derivatives are computed with the PS method. The shifted Caputo fractional derivative is calculated by solving first-order differential equations for quadrature variables, similar to the memory variables used in Zener viscoelasticity. This approach avoids storing the entire particle-velocity history, as done when computing the derivative with the Grünwald-Letnikov approximation. To test the method to ensure visibility of the slow wave, the authors use very high permeability.

Physical stability condition

The first complete calculation of the stability condition for the low-frequency poroelastic equations (no viscous boundary layers in the pores) has been performed by Masson et al. (2006). The algorithm is explicit and has an accuracy of $o(2,4)$ using staggered spatial grids.

A necessary condition for stability is that an inertial acceleration term should be present in Darcy's law. This condition is

$$(1 + \Phi)F - \frac{\rho_f}{\rho} > 0, \quad \Phi = \frac{\omega J}{2a}, \quad F = \frac{T}{\phi}, \quad (5)$$

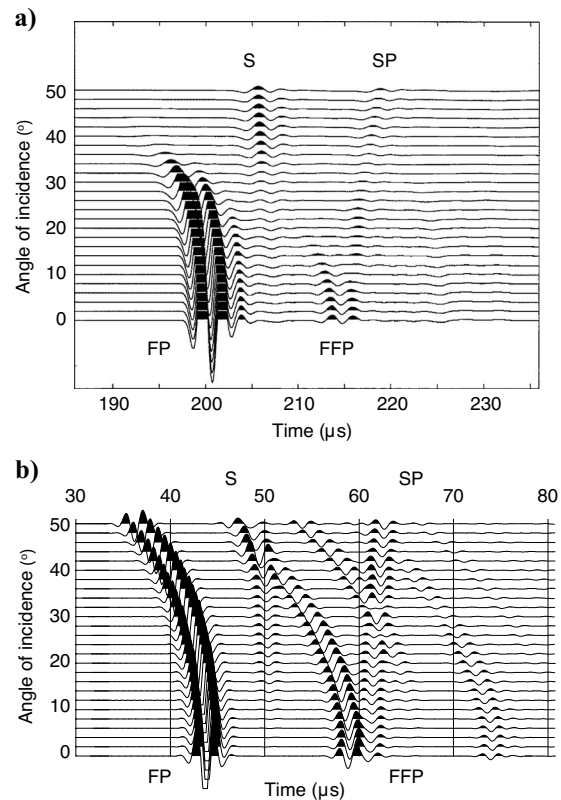


Figure 2. (a) Real microseismogram compared to (b) a numerical simulation obtained from Biot's poro-viscoelastic theory. The events are the fast compressional wave (FP), the shear wave (S), the first multiple reflection of the fast compressional wave (FFP), and the slow wave (SP).

using the notation of that paper, where F is the electrical formation factor. A comparison of this algorithm with the time-splitting method is performed, showing that for comparable time steps, the latter is less accurate at low frequencies. Note that in the case solved by Carcione and Quiroga-Goode (1995) and Wenzlau and Müller (2009) (see below), condition 5 is $(T/\phi) - (\rho_f/\rho) > 0$, i.e., ignoring Φ in that equation, which is equivalent to $\rho m - \rho_f^2 > 0$ (see equation 4; $\lambda > 0$ implies an exponentially growing solution). Using the values given in Table 1, the condition is $7.2 > 0$; generally, stability is satisfied for any realistic rock. For a fluid, $T = 1$, $\phi = 1$, $\rho = \rho_f$, and $\rho m - \rho_f^2 = 0$, which constitutes a limit value. Masson et al.'s (2006) low-frequency code has been used to simulate quasi-static poroelastic propagation resulting from fluid-volume injection source (a Heaviside function in time) compared to an asymptotic semianalytical approach (Vasco, 2008).

The generalization proposed by Masson and Pride (2010) of Biot's equations to describe all the frequency range (as in Lu and Hanyga, 2004) is based on an analytical inverse Fourier transform of the dynamic permeability. The following equation is equivalent to equation 1b:

$$\rho_f \dot{v} + m \dot{q} = -\partial_x p_f - \left(\frac{\eta}{\kappa} \right) \psi * (\dot{q} + a q), \quad (6)$$

$$\psi(t) = \frac{H(t) \exp(-at)}{\sqrt{\pi a t}},$$

where the asterisk denotes time convolution and H is the Heaviside function. This convolution is solved by a time discretization requiring the storage of less than 20 past values. The presence of the convolution makes the scheme more physically stable because it adds to the inertia term $(T/\phi) - (\rho_f/\rho)$ a positive quantity. If $T/\phi \gg 1$, the Courant condition in 1D space is $dt < 0.86(dx/v_p)$, where v_p is the fast P-wave velocity. Spatial discretization is based on a fourth-order FD staggered operator.

Simulation of the seismoelectric effect

Biot's poroelastic equations are the basis of the seismoelectric theory together with Maxwell's electromagnetic equations (Haines and Pride, 2006; Carcione, 2007). Seismic waves generate a 1D force $F = -(\partial_x p_f + \rho_f \dot{v})$ that transports the diffusive charges in the fluid relative to the bound charges in the grains, creating a streaming electric current LF , where L is the coupling coefficient. The bound and diffusive charges are called the electric double layer. This phenomenon is known as *electrofiltration*. On the other hand, an electric field induces a conduction current, according to Ohm's law, and a body force on the excess charge of the diffuse double layer, resulting in fluid filtration. This phenomenon is known as *electro-osmosis*.

Haines and Pride (2006) solve the low-frequency Biot's and Maxwell's equations, neglecting the electro-osmotic effect. The Maxwell equation to solve is then $\nabla \times \mathbf{H} = \sigma \mathbf{E} + L(\eta/\kappa)\mathbf{q}$, where \mathbf{H} is the magnetic field, \mathbf{E} is the electric field, σ is the conductivity, and \mathbf{q} is the grain/fluid relative velocity. The effects of induction can be neglected. This implies $\nabla \times \mathbf{E} = 0$ and thus $\mathbf{E} = -\nabla \varphi$, where φ is the electric potential. Taking the divergence of Maxwell's equations gives Poisson's equation:

$$\nabla \cdot (\sigma \nabla \varphi) = \nabla \cdot \left(\frac{L\eta}{\kappa} \mathbf{q} \right). \quad (7)$$

First, the poroelastic equations are solved by using the algorithm described in Özdenvar and McMechan (1997). Finally, equation 7 is discretized with a second-order FD approximation, leading to a linear system that is solved by conjugate-gradient iterations and improving the conditioning with the helix-derivate concept.

Mesoscopic loss mechanism and quasi-static tests

Masson and Pride (2007) simulate mesoscopic attenuation and dispersion at seismic frequencies using their FD code. Applying stress steps to numerical samples of rocks, we can compute the complex moduli by measuring the strains. The samples are much smaller than the pulse wavelength.

Consider a 2D sample in the (x,z) -plane under plane strain conditions $\epsilon_{yy} = 0$, with the fluid particle-velocity variation set to zero ($v_f = v$) at the edges of the mesh (undrained conditions). The scheme is $\mathcal{O}(2,2)$ at the edges of the mesh to better describe these boundary conditions. From Hooke's law for poroelastic media,

$$\lambda + \mu = \frac{1}{2} \left(\frac{\sigma_{xx} + \sigma_{zz}}{\epsilon_{xx} + \epsilon_{zz}} \right) \quad \text{and} \quad \mu = \frac{1}{2} \left(\frac{\sigma_{xx} - \sigma_{zz}}{\epsilon_{xx} - \epsilon_{zz}} \right), \quad (8)$$

where σ denotes stress and where λ and μ are the (undrained) Lamé constants. The complex bulk modulus is

$$K = \lambda + \frac{2}{3}\mu. \quad (9)$$

The phase velocity and Q are then obtained from

$$v_p = \left[\text{Re} \left(\frac{1}{v_c} \right) \right]^{-1} \quad \text{and} \quad Q = \frac{\text{Re}(v_c^2)}{\text{Im}(v_c^2)}, \quad (10)$$

where v_c is the complex velocity and Re and Im denote real and imaginary parts, respectively (e.g., Carcione, 2007; pp. 321–384). For P- and S-waves, $\rho v_c^2 = \lambda + 2\mu = K + (4\mu/3)$ and $\rho v_c^2 = \mu$, respectively. The method requires four fourth-order spatial differencing points in the smaller patch to avoid numerical artifacts. The numerical experiments show that attenuation is proportional to the square of the incompressibility contrasts and that pure shear attenuation can be caused by fluid exchanges between anisotropically shaped inclusions and the background matrix.

The last significant work using the FD method, where loss from mesoscopic heterogeneities is investigated, is performed by Wenzlau and Müller (2009), who solve the 2D low-frequency particle-velocity–stress formulation of Biot's equations using staggering in time and the standard fourth-order staggered mesh or the rotated staggered grid to compute the spatial derivatives. These workers test the numerical solution in the wave regime of the Biot slow mode and verify the physics of the mesoscopic loss mechanism by means of the above-described long-wavelength experiments. Moreover, they compute the normal-incidence reflection coefficient at a gas-water contact and find that the error is maximum at intermediate frequencies where the slow wave is not sampled properly. At low frequencies, the estimate is acceptable even if the diffusion scale is not resolved properly.

The importance of modeling the slow mode at interfaces is shown by [Chiavassa et al. \(2009\)](#), who use the time-splitting method and a 1D FD $\mathcal{O}(4,4)$ solver with grid refinement at the material contrasts. They explicitly satisfy the interface conditions, and refinements up to 64 times the standard grid size are necessary.

Digital rock physics

A promising field of research is digital rock physics, which combines microscopic imaging with numerical simulations at the micro-scale using direct methods, explicitly discretizing the pore network. Digital rock samples are generated by the so-called open-cell Gaussian random field, where the pore space is defined by the intersection of two two-cut Gaussian random fields. Permeability can be determined through the Lattice-Boltzmann flow simulations on these synthetic digital rocks ([Keehm, 2003](#)). [Saenger et al. \(2007\)](#) provide an outline of the work in progress. In particular, these workers use the rotated staggered-grid FD method to solve the viscoelastic dynamic equations. A viscous fluid based on the generalized Maxwell body describes the loss effects. Insufficient sampling of the viscous boundary layers at the pore walls generates incorrect solutions at low viscosities. At least three grid points are necessary to discretize the skin depth $\delta = (2\eta/\omega\rho_f)^{1/2}$. Propagation through a fluid/porous-medium interface shows that the slow wave is only generated if there is hydraulic contact at the interface (open-pore conditions) (e.g., [Carcione, 2007](#); pp. 284–288).

An approach to explicitly model cracks and fractures is proposed by [Zhang and Gao \(2009\)](#). The scheme treats the fractures as non-welded interfaces that satisfy the linear-slip displacement-discontinuity conditions instead of using equivalent medium theories. The discretization is based on tetrahedrons, and arbitrary 2D nonplanar fractures can be incorporated accurately into the numerical mesh. The modeling allows the background media to differ on both sides of the fracture. Hence, the algorithm can be used to characterize the seismic response of fractured media and to test equivalent medium theories.

Double-porosity equations

A recent Biot-type poroelastic theory treats the mesoscopic loss created by lithological patches having, for example, different degrees of consolidation. It is called the double-porosity model (e.g., [Pride et al., 2004](#)). There are two phases, and the theory explicitly considers the field variables of these phases. [Ba et al. \(2008\)](#) have solved the governing equations (homogeneous case) using the splitting method introduced by [Carcione and Quiroga-Goode \(1995\)](#). A dimensionless quantity $\zeta = \gamma^*(p_{f1} - p_{f2})$ couples the two phases and represents the mesoscopic flow, i.e., the average rate at which fluid volume is transferred from phase 1 into phase 2, where γ has the frequency dependence $(1 - (i\omega/\omega_m))^{1/2}$ and ω_m is a resonance frequency. The approach implemented by [Ba et al. \(2008\)](#) to solve the convolution is to use first-order FD in time and an explicit discrete time Fourier transform.

[Liu et al. \(2009\)](#) solve equivalent poroviscoacoustic equations by approximating the mesoscopic complex moduli in the frequency domain using Zener mechanical models, in the same way as [Carcione \(1998\)](#) represents the Biot loss mechanism. The equations are then solved in the time domain using memory variables and the splitting method.

Modeling the diffusive Biot mode

Recently, [Carcione and Gei \(2009\)](#) solve the equation describing the diffusion of the slow static mode in anisotropic media with a time-domain spectral solver, which has high temporal accuracy and allows the use of coarse numerical meshes. A correction to the stiffness of the rock under conditions of transverse isotropy and uniaxial strain is assumed to model borehole conditions. The algorithm has been tested with the Green's function and applied to pressure diffusion in fractal permeability media, simulating realistic reservoir conditions. The simulations show that the energy velocity must be used to track the diffusion front.

FINITE-ELEMENT METHODS

The FE method is based on a variational formulation of the equations of motion 1. Among its advantages is the ability to fit discontinuities employing irregular meshes and the use of polynomials of arbitrary degree. Also, it allows easy implementation of natural and mixed boundary conditions. Furthermore, because the FE approximate solutions are sought in spaces of functions consisting of piecewise polynomials of a chosen degree k , the functional-analysis tools are available to derive a priori error estimates for the algorithms. This gives asymptotic bounds for the distance between the solutions of the differential model and the computed solution — measured in the L^2 -norm or more generally in a Sobolev norm ([Adams, 1975](#)) — in terms of mesh size and polynomial degree.

Space–time-domain solution of Biot's equations

Let us denote by $H^1(\Omega)$ the Sobolev space of functions in $L^2(\Omega)$ having first derivatives in $L^2(\Omega)$, whereas $H(\text{div}, \Omega)$ is the space of vector functions in $[L^2(\Omega)]^d$ with divergence in $L^2(\Omega)$ (d is the Euclidean dimension). The existence, uniqueness, and regularity of the solution of Biot's equations of motion in a bounded domain Ω under Neumann boundary conditions are analyzed by [Santos \(1986\)](#); continuous and discrete time FE Galerkin procedures are presented in [Santos and Oreña \(1986\)](#). These works show that for each time t , the solid and fluid displacement vectors belong to the spaces $[H^1(\Omega)]^d$ and $H(\text{div}, \Omega)$, respectively, which in turn yield appropriate choices for the FE spaces to compute approximate solutions. More specifically, conforming approximations to the solid displacement must be sought in FE spaces having global continuity; conforming spaces to compute the fluid displacement are only required to satisfy continuity of the normal component at the interior faces of the computational mesh. For a mesh size h and a time step dt , optimal a priori error estimates in the energy norm of the form $O(dt^2 + h^k)$ are derived.

The results given in [Santos \(1986\)](#) are extended in [Santos et al. \(1988a\)](#) and [Lovera and Santos \(1988\)](#), where FE methods to simulate wave propagation in an elastic solid containing a Biot medium are developed and analyzed. The coupled motion of a compressible inviscid fluid with a Biot medium in a cylindrically symmetric domain to compute full-waveform acoustic logs is simulated in [Santos et al. \(1988b\)](#). A quadrature rule is used to define an explicit FE procedure. A first-order absorbing-boundary condition for Biot's media is also derived. [Douglas et al. \(1991b\)](#) model synthetic logs using this technique. The method is also used to simulate the slow P-wave in Biot media at ultrasonic frequencies and the scattering of this wave in real rocks resulting from the presence of mesoscopic heterogeneities ([Douglas et al., 1991a](#); [Hensley et al., 1991](#)).

Teng (1990) uses the Galerkin weighted residual process with regular cells to obtain the nodal equations of motion. Moreover, the use of an explicit FD time solver makes the technique efficient in terms of computer time because one may avoid matrix inversions. Teng's simulation at fluid/poroelastic interfaces satisfying open and sealed boundary conditions agrees with experimental data.

Generalized Biot models for immiscible fluids and composite porous solids

Santos et al. (1990a, 1990b) extend Biot's theory to the case in which the porous medium is saturated by two immiscible, compressible, viscous fluids (wetting/nonwetting system). The model takes into account capillary-pressure effects using a Lagrange multiplier in the complementary virtual work principle. It is assumed that the relative flow of the fluid phases is laminar and causes energy losses attributable to a dissipation potential implemented in the Lagrangian formulation of the equations of motion.

Gedanken experiments to determine the seven elastic coefficients in the constitutive relations are presented. A plane-wave analysis predicts one shear (S-wave) and three compressional waves: a fast P-wave corresponding to the motion in phase of the solid and fluid phases and two slow P-waves associated with motions out of phase of the two fluids. An extension of this model to include in situ conditions of the single phases and viscoelasticity is given in Ravazzoli et al. (2003) and Ravazzoli and Santos (2005), with a parametric analysis of the influence of effective pressure, abnormal pore pressure, and saturation on the phase velocities and Q factors of the different waves.

The first numerical evidence of the presence of a second slow wave in porous solids saturated by immiscible fluids is presented in Santos et al. (2002) and Santos et al. (2004b). They show that the second slow wave can be detected at ultrasonic frequencies, but at low frequencies this wave is a source of attenuation of the fast waves (the mesoscopic loss).

Partially frozen porous media and shaly sandstones are particular cases of fluid-saturated porous media when the solid matrix is composed of two weakly coupled solids. Leclaire et al. (1994) develop a Biot model valid only for uniform porosity. A generalized model valid for the variable porosity case is presented in Santos et al. (2004a), thus allowing one to perform numerical simulations in realistic situations. Three compressional waves (one fast and two slow) and two shear waves (one fast and one slow) propagate in this type of medium.

Using an alternative approach based on first principles at the microscale, the two-space homogenization technique (Sanchez Palencia, 1980) is used in Santos et al. (2005) and Santos and Sheen (2008) to obtain the equations of motion and a generalized Darcy's law in fluid-saturated composite porous solids. The resulting macroscale equations are similar to those derived by Carcione et al. (2003b) and Santos et al. (2004a).

The analysis of the reflection and transmission coefficients at interfaces within composite porous media is presented in Rubino et al. (2006a), concluding the importance of slow-wave conversions at interfaces defined by a contrast in ice content in partially frozen sandstones.

Space-frequency-domain solution of Biot's and Biot-type equations

The space-frequency formulation of Biot's equations of motion and its generalization is a convenient way to include intrinsic losses

and frequency-dependent mass and viscous coupling coefficients, avoiding the need for performing time convolutions. The foundations of this approach are presented in Douglas et al. (1993), where a priori error estimates in terms of the mesh size h and the angular frequency ω are first derived. The idea is to solve the Helmholtz equations for a finite number of angular frequencies and then obtain the space-time solution using an inverse-time Fourier transform.

Numerical dispersion is an important aspect to be analyzed when solving wave-propagation problems. Zyserman et al. (2003) show that the nonconforming elements presented in Douglas et al. (1999) need about half the number of points per wavelength to achieve a desired tolerance in numerical dispersion as compared with the standard conforming bilinear elements. Based on this conclusion, Zyserman and Santos (2007) perform a numerical dispersion analysis of a FE procedure to solve Biot's equations. They use the nonconforming elements of Douglas et al. (1999) to represent each component of the solid displacement and the vector part of the Raviart-Thomas-Nedelec space of zero order (Raviart and Thomas, 1977; Nedelec, 1980) to represent the fluid-displacement vector. The local degrees of freedom for the solid and fluid displacements in rectangular or triangular elements are located at the centers of the faces of the elements, defining a staggered mesh. The analysis gives lower bounds for the number of points per wavelength of the slow wave in order to have a negligible error in the group velocities of the fast waves.

Santos and Sheen (2007) use the FE spaces described by Zyserman and Santos (2007) to solve the equations of motion given in Santos et al. (2004a) with a collection of global and iterative domain-decomposed FE methods. The algorithm includes an implementation of absorbing-boundary conditions. The analysis yields optimal a priori error estimates and convergence results for the domain-decomposition iteration. Numerical experiments showing the propagation of the five types of waves in a partially frozen sandstone are also presented.

The domain-decomposition iteration of Santos and Sheen (2007) is also used by Rubino et al. (2008) to simulate the acoustic response of gas-hydrate-bearing sediments in a research exploration well. The simulations are performed assuming the presence of multiscale spatial heterogeneities associated with zones of low and high gas-hydrate saturations. The levels of attenuation in the synthetic traces are in excellent agreement with those measured at the well, showing that multiscale distributions of gas hydrates may explain the observed attenuation.

The P-wave attenuation by slow-wave diffusion caused by mesoscopic-scale heterogeneities is a significant loss mechanism at low frequencies. Rubino et al. (2006b) and Picotti et al. (2007) implement an iterative FE domain-decomposition iteration in a parallel computer, similar to that of Santos and Sheen (2007), to model wave propagation at seismic frequencies in a periodically stratified medium. The Q factors obtained from the synthetic traces, estimated with spectral-ratio and frequency-shift methods, are in very good agreement with those predicted by White's theory.

Using a reduced Biot model that ignores the shear and slow P-waves, Bermudez et al. (2006) present a displacement/pressure poroelastic FE method to compute the response to a harmonic excitation of a 3D enclosure containing a fluid and a poroelastic material. For a tetrahedral mesh, they use the lowest-order Raviart-Thomas-Nedelec space for the fluid and the sum of a bubble and a polynomial of the first degree for the solid.

Oscillatory tests in the space-frequency domain

Numerical simulations using Biot equations of motion in the presence of mesoscopic-scale heterogeneities require extremely fine meshes to properly represent these heterogeneities and their attenuation effects on the fast waves. An alternative approach to wave propagation is to use a numerical upscaling procedure to determine an equivalent viscoelastic solid to the original Biot medium (Rubino et al., 2009; Santos et al., 2009), using the computer as a virtual laboratory. The procedure consists of simulating oscillatory compressibility and shear tests in the space-frequency domain to determine the equivalent (complex) undrained P- and S-wave moduli on a representative sample at a finite number of frequencies. The sample is assumed to obey Biot's equations of motion, and the FEM is used to solve the associated boundary-value problems.

In general, the distribution of the mesoscopic multiscale heterogeneities has a stochastic nature, so the oscillatory tests are applied in a Monte Carlo fashion on many realizations of the stochastic heterogeneities. Computing the moments of the equivalent phase velocities and inverse Q factors yields the desired equivalent viscoelastic medium. The procedure allows us to determine the complex moduli for arbitrary spatial distributions of the heterogeneities, where no analytical solutions are available.

Figure 3 displays an oscillatory compressibility test applied to a representative sample of partially saturated poroelastic material. Such spatial distribution of fluids may occur when shale strings seal off local pockets of gas, creating many gas-liquid contacts, or during field production, when gas may come out of solution and create distributed pockets of free gas (White, 1975). The boundary conditions are a normal stress applied to the top boundary [$\Delta P \exp(i\omega t)$], and no tangential external forces are applied to the top and lateral boundaries. The fluid is not allowed to flow into or out of the sample, and the solid is not allowed to move at the bottom boundary nor to have horizontal displacements at the lateral boundaries of the sample. The domain is a square measuring 50 cm per side. Overall gas saturation is 10%. Black zones correspond to pure gas saturation and white zones to pure brine saturation (Figure 3a). The number of cells is 75×75 .

Figure 3b shows the normalized fluid pressure at a frequency of 50 Hz. The fluid-pressure gradients are maximum at the boundaries of the gas patches, producing fluid flow and Biot slow waves that diffuse away from the gas-water interfaces generating energy losses and velocity dispersion (mesoscopic losses). The value of the P-quality factor is approximately six at 50 Hz, so there are significant attenuation and dispersion effects because of the diffusive Biot waves generated at the boundaries of the gas patches. This strong attenuation may occur in reservoir sandstones subject to overpressure or in unconsolidated ocean sediments.

Simulation of coupled seismic and electromagnetic waves

As explained earlier, seismic waves propagating through near-surface layers of the earth may induce electromagnetic disturbances that can be measured at the surface (seismoelectric effect, electrofiltration) (Pride and Haartsen, 1996; Mikhailov et al., 1997). Recent tests suggest that the reciprocal process, i.e., surface-measurable acoustic disturbances induced by electromagnetic fields (electroseismic effect, electro-osmosis), is also possible (Thompson, 2005; Hornbostel and Thompson, 2007). To explain these phenomena, Thompson and Gist (1993) and Pride (1994) suggest they are

generated by an electrokinetic coupling mechanism. Using a volume-averaging approach, Pride (1994) derives a set of equations describing electroseismic and seismoelectric effects in electrolyte-saturated porous media. In these equations, the coupling mechanism acts through the (generally frequency-dependent) electrokinetic coupling coefficient L (see equation 7). When this coefficient is set to zero, Pride's set of equations turns to the uncoupled Maxwell's and Biot's equations.

Santos (2009) presents a collection of 2D FEMs for the space-frequency domain solution of the fully coupled Pride's equations in a bounded domain, including absorbing boundary conditions. If only seismic sources are present, the electro-osmosis effects can be neglected and we have a seismoelectric FE model. On the other hand, when only electromagnetic sources are considered, electrofiltration can be ignored, yielding an electroseismic numerical model.

The approach is based on a mixed formulation for Maxwell's equations and a standard Galerkin formulation for Biot's equations

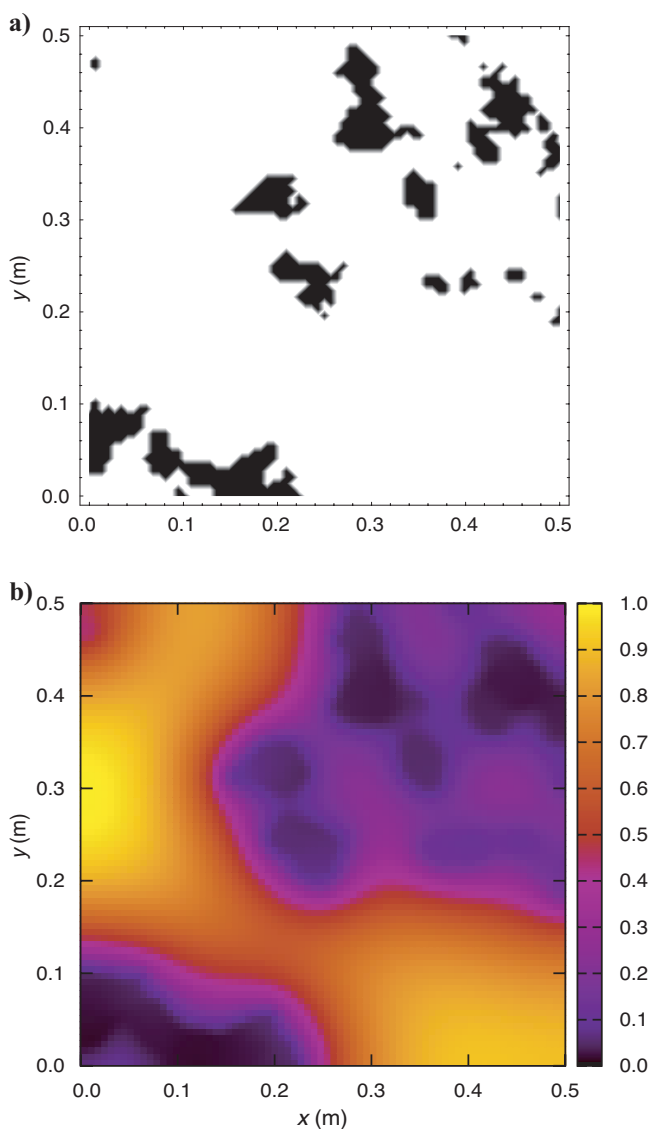


Figure 3. (a) Sample of porous rock with patchy gas-water saturation; (b) normalized fluid-pressure after an oscillatory compressibility test.

in global and domain decomposed forms. The analysis includes existence and uniqueness of the approximate solution, a priori error estimates for the global procedure, and convergence for the domain decomposition iteration. The electric-field vector and the scalar magnetic field, corresponding to the case of compressional and vertically polarized seismic waves coupled with transverse magnetic polarization (PSVTM mode), are computed with the rotated Raviart-Thomas-Nedelec FE spaces of zero order. Each component of the solid-phase displacement vector is approximated by using the nonconforming space defined in Douglas et al. (1999), whereas the displacement in the fluid phase is approximated using the vector part of the Raviart-Thomas-Nedelec mixed FE space of zero order.

The 2D FE spaces for the case of horizontally polarized shear waves coupled with the transverse electric polarization (SHTE mode) are identical to those of the PSVTM mode, except that in this mode the solid and fluid displacements are scalar functions in H^1 and L^2 , respectively. Consequently, the solid displacement is approximated using the nonconforming spaces defined in Douglas et al. (1999) and the fluid displacement employing piecewise constants. Recently, numerical experiments incorporating the algorithms presented in Santos (2009) are used in Zyserman et al. (2010) to model PSVTM and SHTE electroseismics.

Discontinuous Galerkin method

Several forms of the discontinuous Galerkin method (DGM) have been applied to acoustic and elastic wave equations. Early formulations of the DGM for elliptic problems can be found in Wheeler (1978). A locally implicit space-time DGM [ADER-DG(ST)] using numerical fluxes on unstructured tetrahedral meshes is presented by de la Puente et al. (2008) to solve Biot's equations on 3D bounded domains. The formulation is valid for inviscid fluids and the low-frequency case, and the algorithm is validated by comparison with known analytical and numerical solutions.

De Basabe et al. (2008) give a numerical dispersion analysis for an interior penalty DGM for elastic wave propagation, suggesting that Lagrange basis functions combined with Gauss quadratures is a good choice for wave-propagation simulations (see De Basabe and Sen [2007] and references therein for grid-dispersion analysis of FEM).

SPECTRAL FINITE-ELEMENT METHODS

The SE method was pioneered in the late 1980s by Patera (1984) and Maday and Rønquist (1990), and it was used successfully in computational fluid dynamics before generating interest for seismic wave-propagation problems. In the time domain, SE methods have shown high accuracy for 2D and 3D elastic wave modeling (e.g., Seriani et al., 1992; Komatitsch and Vilotte, 1998) as well as for anisotropic and anelastic effects (Komatitsch et al., 2000a). Fluid/solid boundaries have also been treated based upon domain decomposition (Komatitsch et al., 2000b; Chaljub et al., 2007). In the frequency domain, SE has appeared to be of high interest for wave propagation in layered structures (Rizzi and Doyle, 1992; Doyle, 1997; Igawa et al., 2004; Baskaran et al., 2006). SE methods have also been used for wave propagation in porous media in the frequency domain (e.g., Degrande and De Roeck, 1992a, 1992b) and the time domain (Morency and Tromp, 2008).

Space–frequency-domain solution of Biot's equations

The governing equations of motion, such as those given by equations 1, are first transformed from the time domain, where coupled partial differential equations need to be solved, to the frequency domain using a Fourier transform that simplifies these equations to a set of coupled ordinary differential equations. The solution is then found by solving a frequency-dependent eigenvalue problem. Degrande and De Roeck (1992a) solve the 1D Biot equations in terms of solid and relative fluid displacements. They apply their implementation to the resolution of a transient pulse propagating through a saturated porous column. For this exercise, they use high permeability. Doing so, they are able to observe the propagation of the two compressional waves as well as their attenuation. They expand this implementation to 2D wave propagation in layered saturated media (Degrande and De Roeck, 1992b).

In another paper, Degrande et al. (1998) tackle the problem of wave propagation in a coupled dry, saturated, and unsaturated porous medium, here again in a layered structure. Subsequently, they present a series of applications mimicking (1) the effect of a moving water table on the propagation of transient waves in an isotropic axisymmetric half-space and (2) the influence of air bubbles in the pores of an unsaturated medium. Because of their formulation, the mass distribution and the stiffness matrix are calculated exactly. The number of elements in this case coincides with the number of discontinuities (layers) in the model.

Space–time-domain solution of Biot's equations

To our knowledge, Morency and Tromp (2008) are the first to solve the Biot equations with SEM for the solid and relative fluid displacements in the time domain. They present a general 3D implementation accounting for porosity discontinuity.

Discretization, assembly, and time marching

Similar to finite-element methods, a mesh is designed representing a subdivision of the model volume Ω into n_{el} nonoverlapping finite elements (quadrilateral in 2D space and hexahedral in 3D space) Ω_e , $e = 1, \dots, n_{el}$, at which level the partial differential problem is approximated. Each of these elements is mapped to a reference domain $[-1, 1]^{n_d}$ (for a square in two dimensions, $n_d = 2$; for a cube in three dimensions, $n_d = 3$). Therefore, a unique relationship exists between a point \mathbf{x} within Ω_e and a Gauss-Lobatto-Legendre (GLL) integration point ξ in the reference domain. These GLL points are the roots of $(1 - \xi^2)P'_{n_l}$, where P_{n_l} is a Legendre polynomial of degree n_l . The Lagrange polynomials $l_\alpha^{n_l}$ of degree n_l , associated with $n_l + 1$ GLL control points ξ_α within $[-1, 1]$, with $\alpha = 0, \dots, n_l$, are such that at any control point ξ_β , the Lagrange polynomials return zero or one, that is, $l_\alpha^{n_l}(\xi_\beta) = \delta_{\alpha\beta}$. This property leads to an important result on the mass matrices.

Contrary to the FE method, the SE method relies upon the use of higher-degree Lagrange polynomials to interpolate functions on the elements. In SE wave propagation, one typically uses a polynomial degree n_l between 4 and 10 (Komatitsch and Vilotte, 1998). On each volume element Ω_e , any function f is interpolated by triple products (in 3D problems) of Lagrange polynomials as

$$f(\mathbf{x}(\xi, \eta, \zeta)) \sim \sum_{\alpha, \beta, \gamma} f^{\alpha\beta\gamma} l_\alpha^{n_l}(\xi) l_\beta^{n_l}(\eta) l_\gamma^{n_l}(\zeta), \quad (11)$$

where $f^{\alpha\beta\gamma}$ refers to the value of f at the interpolation point $\mathbf{x}(\xi_\alpha, \eta_\beta, \zeta_\gamma)$. Consequently, the SE method retains the ability of the FE method to handle complex geometries while keeping the strength of exponential convergence and accuracy resulting from the use of high-degree polynomials. One crucial advantage of the method is that, for acoustic, elastic, and poroelastic equations, the mass matrices are diagonal, which naturally unfolds from the use of high-degree Lagrange interpolants and the GLL integration rule. This makes the SE solver very well suited for parallel computation, as shown by Fischer and Rønquist (1994) and Komatitsch et al. (2002).

Finally, because the mass matrices are diagonal, the system can be solved based on a simple explicit time-marching scheme, e.g., the Newmark scheme using a predictor/multicorrection technique.

The key element in poroelastic wave-propagation modeling is to resolve the slow P-wave accurately, which can be diffusive (at low frequency) or can propagate at a much slower speed than the fast P- or S-waves (at high frequency). Accuracy and stability for SE calculations are determined by ensuring a minimum of five grid points per shortest wavelength and a Courant number lower than 0.3, as experimentally estimated for elastic waves using a regular mesh (see Komatitsch, 1997).

Boundary conditions and material discontinuities

A surface integral accounting for boundary conditions, first-order material discontinuities, and absorbing conditions naturally arises in the weak-form equations, obtained by dotting each of the two governing equations with arbitrary test vectors and integrating over the model volume, which is standard in FE methods.

Free surface, corresponding to zero tractions, is accommodated when the integral of the tractions along this boundary vanishes. To simulate unbounded media, outgoing waves need to be absorbed. Morency and Tromp (2008) use a classical first-order absorbing boundary condition based upon a paraxial approximation (see, e.g., Clayton and Engquist [1977] for details).

Material discontinuities in a porous medium in terms of moduli, densities, permeability, and viscosity are naturally taken into account by the method. SE methods imply continuity of displacements between common edges of elements by construction. However, the relative fluid displacement with respect to the solid skeleton is weighted by the porosity, which breaks the displacement continuity for sharp discontinuity in porosity. As shown by Morency and Tromp (2008), sharp discontinuity in porosity can be treated by domain decomposition. They also show that smooth gradients in porosity are in turn naturally taken into account by the method. One needs also to realize that discontinuity within an element, from one GLL point to another, is fully acceptable.

Coupled wave propagation within an acoustic and poroelastic or elastic and poroelastic medium is also treated by Morency and Tromp (2008), using domain decomposition. Each domain is treated separately, and coupling is achieved by ensuring continuity of displacement and traction at the boundary. A comparison between analytical solutions derived by a Cagniard de Hoop method (Diaz and Ezziani, 2010) and SEM solutions shows good agreement for the acoustic/poroelastic coupling, as seen in Figure 4. This simulation is an idealized example because friction is neglected. The experiment is improbable in the real world, but it is useful for testing the code. An explosive source is used with a Ricker wavelet source time function, situated in the upper acoustic half-space (cross), and we consider a receiver in each layer (triangles). The snapshot of the vertical

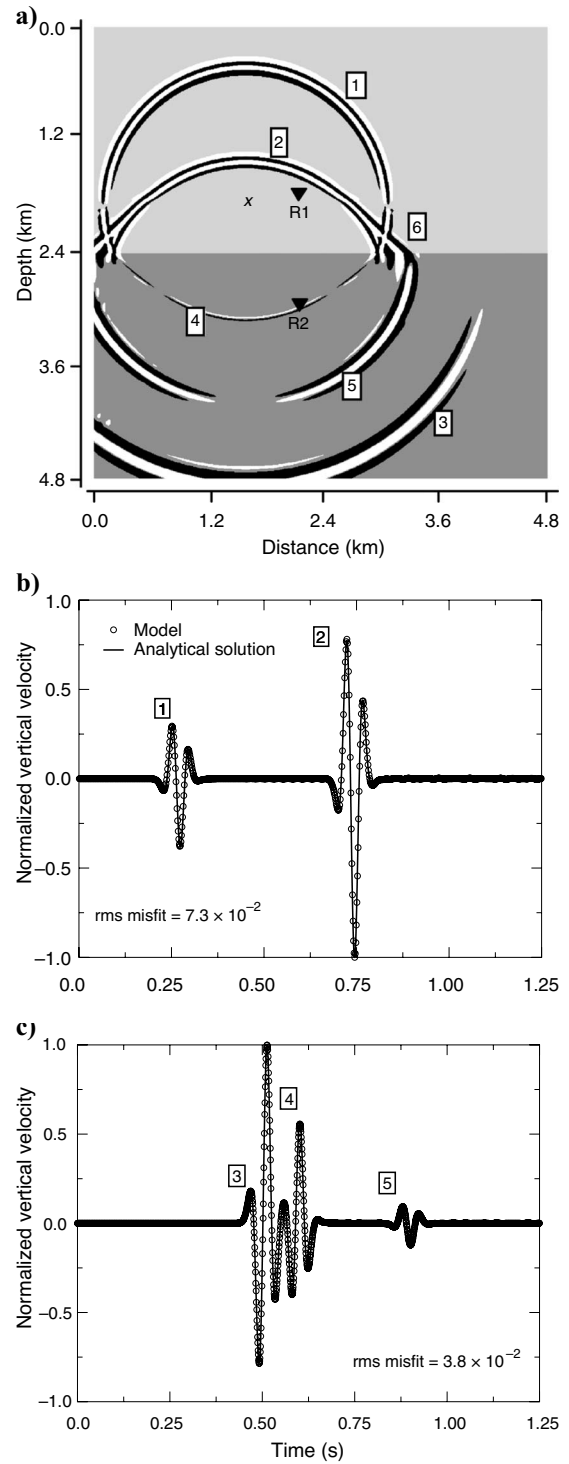


Figure 4. Wave propagation in a coupled acoustic/inviscid poroelastic medium: (a) snapshot of the solid displacement vertical-component. SEM seismograms and analytical solutions comparison at (b) receiver R1 in the acoustic domain and (c) receiver R2 in the poroelastic domain (modified after Morency and Tromp, 2008). 1 = direct P-wave in the acoustic layer; 2 = reflected P-wave in the acoustic layer; 3 = transmitted fast P-wave; 4 = P-to-S wave; 5 = fast-to-slow P-wave; 6 = refracted S-to-P-wave in the acoustic layer.

component of the displacement in Figure 4a displays the direct and reflected P-waves in the acoustic layer and the transmitted fast P-wave, the P-to-S wave, and the fast P- to slow P-wave in the poroelastic layer. We also notice a head wave in the acoustic layer, as the refracted S-to-P-wave. Figure 4b and c compares analytical solutions (solid line) and SEM vertical-component velocity seismograms (circles) at receivers R1 in the acoustic layer and R2 in the poroelastic layer, respectively. The corresponding rms misfit values on each plot show good agreement between numerical and analytical solutions.

Attenuation effects

Morency and Tromp (2008) treat effects associated with physical dispersion and attenuation and frequency-dependent viscous resistance based upon a memory variable approach. The equation 1b is then replaced by

$$\rho_j \ddot{v} + m \dot{q} + b(t) * q = - \partial_x p_f. \quad (12)$$

The function $b(t)$ takes into account the frequency dependence of the fluid-flow regime. At low frequency, the flow regime is of Poiseuille (laminar) and the slow P-wave is diffusive, with $b = \eta / \kappa$. At high frequency, inertial forces dominate the flow regime and the slow P-wave propagates. In that case, the relaxation function $b(t)$ may be described in terms of viscous relaxation mechanisms (see Carcione [2007] and Morency and Tromp [2008] for details).

A similar approach is used to account for the anelastic response of the frame. In that case, a viscoelastic rheology is introduced (e.g., Carcione, 2007).

Hierarchical FE techniques

Hierarchical FE techniques have been developed using high-order polynomials, referred to as hierarchical functions, to describe displacement fields (Houmat, 1997). One characteristic of these hierarchical techniques is the possible use of different polynomial orders for the different displacement components. These techniques have been used successfully to model wave propagation in air-saturated foam material used in aircraft and ground transportation vehicles for thermal insulation and sound absorption. Hörlin et al. (2001) present a convergence analysis in the case of a homogeneous porous layer. The general trend is that for higher frequencies, a higher polynomial degree is required. Notice that the flow resistivity of a foam is on the order of $10^3 \text{ kg}/(\text{m}^3 \text{ s})$, almost seven orders of magnitude smaller than the resistivity of oil in a reservoir.

In a later paper, Hörlin (2005) introduces a 3D hierarchical hp-FE implementation of Biot's equations, adopting a combination of higher-order polynomials for the element base functions and mesh refinement. He finds that fourth- or fifth-order polynomials for mesh refinement are the most computationally efficient to achieve a level of the results, which is of interest from an engineering application point of view characterized by a low-frequency regime. However, the case of a two-porous-layers problem shows some slow convergence of the fluid displacement at the interface, which is solved by increasing the coupling between the solid and fluid phases, i.e., increasing the flow resistivity. Looking at a multilayer geometry, Göransson (2006) manages to reach an accuracy better than 10% in the displacements and fluid pressures using higher-order polynomials.

INVERSE PROBLEMS

As we have described, the poroelastic forward problem has been solved using different numerical techniques. The inverse problem, on the other hand, is rarely addressed. Inverse procedures are based upon characterizing the sensitivity of the seismic wavefield to perturbations in the model parameters through sensitivity kernels, or Fréchet derivatives (Tarantola, 1984, 1987). They are of high interest to derive material properties from a measured signal.

To our knowledge, the first work done in this area has been by De Barros and Dietrich (2008). The authors derive Fréchet derivatives in terms of the Green's functions of a 1D reference medium based upon a perturbation analysis of the poroelastic wave equations in the plane-wave domain using the Born approximation. In this study, two series of Fréchet derivatives are defined in terms of the fluid and bulk densities, and the Biot coefficients, as well as in terms of the solid- and fluid-phase densities, permeability, porosity, solid and fluid bulk moduli, solid shear modulus, and a consolidation coefficient. De Barros and Dietrich present a detailed sensitivity study to investigate the influence of a small perturbation of each model parameter on the seismic wave. They conclude that, with their formulation, inversion for porosity and the consolidation coefficient is more manageable than for permeability.

Morency et al. (2009) present a general 3D derivation of finite-frequency sensitivity kernels based upon SE and adjoint methods. The authors extend work done in (an)elastic wave propagation (e.g., Tarantola, 1987; Tromp et al., 2005; Liu and Tromp, 2008) to porous media. In this study, the workers present three series of Fréchet derivatives. The first series is defined in terms of the eight parameters appearing in the Biot equations. A second series offers a parameterization in terms of density-normalized moduli corresponding to squared wavespeeds. The last series involves the poroelastic shear and compressional wavespeeds as well as the porosity and permeability. A gallery of 2D finite-frequency sensitivity kernels is presented, which illustrates the sensitivity of the fast and slow compressional waves and the shear wave to the poroelastic parameters. As with De Barros and Dietrich (2008), Morency et al. (2009) observe the weak sensitivity to the permeability for their choice of misfit function. A possible use of electrokinetic effects to improve permeability characterization is succinctly mentioned at the end of their paper.

Connections have been drawn between imaging in exploration seismology, adjoint methods, and finite-frequency tomography in the context of onshore and offshore elastic modeling by Luo et al. (2009) and Zhu et al. (2009). They demonstrate that the density sensitivity kernel in adjoint tomography is closely related to the imaging principle in exploration seismology introduced by Claerbout (1971). They also show that in elastic modeling, reflectors are better characterized by the impedance kernel. It is thus natural to expect that in poroelastic modeling an equivalent to the elastic impedance kernel will arise. Notice, though, that in an isotropic poroelastic medium, there are three types of densities and three wavespeeds, contrary to an isotropic elastic medium that presents one density and two wavespeeds. Several potential impedance kernels may thus be defined in a poroelastic medium.

CONCLUSIONS

We have provided a review of the main direct methods used in dynamic poroelasticity. The algorithms discussed — FE, PS, and FE

methods (low-order FE and SE) — do not have restrictions on the type of constitutive equation, boundary conditions, and source type, and they allow general material variability.

Without simplified assumptions, many of the complex constitutive equations handled by direct methods cannot be solved with ray and analytical methods. Finite differences are simple to program and, under not very strict accuracy requirements, are very efficient. In this sense, a good choice can be a second-order-in-time, fourth-order-in-space FD algorithm. Pseudospectral methods can, in some cases, be more expensive, but they guarantee high accuracy when staggered differential operators are used. In 3D space, pseudospectral methods require a minimum number of grid points, compared to finite differences, and can be the best choice when limited computer storage is available.

The best algorithm to model surface topography and curved interfaces is without a doubt the FE method, which, with the use of high-order interpolators, can also compete in terms of accuracy and stability with the previous techniques. FE and SE methods are also best suited for engineering problems, where interfaces have well-defined geometric features, in contrast with geologic interfaces. Use of non-structured grids, mainly in 3D space, can be challenging and time consuming and it may require complex mesh builders. However, FE and SE methods remain preferred techniques for seismic problems involving the propagation of surface waves in situations of complex topography.

The coexistence of waves and diffusion modes is challenging, mainly because the velocity of the slow modes vary from zero at low frequencies to a finite value at high frequencies and the attenuation level can be very high. The mesoscopic loss mechanism, which involves small heterogeneities compared to the pulse wavelength, can be described by an effective complex modulus and simulated by means of viscoelastic models. The effective compressional and shear moduli can be obtained with harmonic simulations in the frequency domain or quasi-static experiments in the time domain, made on many realizations of stochastic heterogeneities.

Progress has been made in many other aspects: the poroelastic equations have been solved by describing several attenuation mechanisms using viscoelastic models, general material symmetry (anisotropy), partial saturation, and multiphase media such as permafrost. Digital rock physics explicitly considers the microstructure and can be used to perform virtual experiments and to verify effective theories such as Biot's and other macroscopic poroelastic theories. Poroelasticity combined with electromagnetism explains the electrokinetic phenomenon, which in turn yields models to analyze electroseismic and seismoelectric effects that have been simulated by FD and FE methods.

The numerical methods have been tested in unbounded media and in the presence of a material interface, which allows the simulation and analysis of surface and interface waves in poroelastic media. Finally, the inverse problem in poroelastic media is essential to derive material properties, particularly microstructural information, from a measured signal. Recent studies bring promising insights.

ACKNOWLEDGMENTS

We thank Boris Gurevich, Hans Helle, and two anonymous reviewers for useful comments.

REFERENCES

- Adams, R. A., 1975, Sobolev spaces: Academic Press, Inc.
- Aldridge, D. F., N. P. Symons, and L. C. Bartel, 2005, Poroelastic wave propagation with a velocity-stress-pressure algorithm: Proceedings of the Third International Conference on Poromechanics, 253–258.
- Allard, J. F., 1993, Propagation of sound in porous media: Modelling sound absorbing materials: Elsevier Applied Science.
- Arntsen, B., and J. M. Carcione, 2001, Numerical simulation of the Biot slow wave in water-saturated Nivelsteiner Sandstone: *Geophysics*, **66**, 890–896.
- Ba, J., J.-X. Nie, H. Cao, and H.-Z. Yang, 2008, Mesoscopic fluid flow simulation in double-porosity rocks: *Geophysical Research Letters*, **35**, doi: 10.1029/2007GL032429.
- Baskaran, G., K. Balasubramaniam, and C. V. Krishnamurthy, 2006, Simulation of ultrasonic technique using spectral element method, in D. O. Thompson, and D. E. Chimenti, eds., Review of quantitative nondestructive evaluation: 111–117.
- Bermudez, A., J. L. Ferrín, and A. Prieto, 2006, Finite element solution of new displacement/pressure poroelastic models in acoustics: *Computer Methods in Applied Mechanics and Engineering*, **195**, 1914–1932.
- Biot, M. A., 1962, Mechanics of deformation and acoustic propagation in porous media: *Journal of Applied Physics*, **33**, 1482–1498.
- Bourbié, T., O. Coussy, and B. Zinzner, 1987, Acoustics of porous media: Editions Technip.
- Caputo, M., 1969, *Elasticità e dissipazione*: Zanichelli.
- Carcione, J. M., 1996, Wave propagation in anisotropic, saturated porous media: Plane wave theory and numerical simulation: *Journal of the Acoustical Society of America*, **99**, 2655–2666.
- , 1998, Viscoelastic effective rheologies for modeling wave propagation in porous media: *Geophysical Prospecting*, **46**, 249–270.
- , 2007, Wave fields in real media: Theory and numerical simulation of wave propagation in anisotropic, anelastic, porous and electromagnetic media, 2nd ed.: Elsevier Scientific Publ. Co., Inc.
- Carcione, J. M., F. Cavallini, J. E. Santos, C. L. Ravazzoli, and P. M. Gauzelino, 2004, Wave propagation in partially-saturated porous media: Simulation of a second slow wave: *Wave Motion*, **39**, 227–240.
- Carcione, J. M., and D. Gei, 2009, Theory and numerical simulation of fluid-pressure diffusion in anisotropic porous media: *Geophysics*, **74**, no. 5, N31–N39.
- Carcione, J. M., and H. B. Helle, 1999, Numerical solution of the poroviscoelastic wave equation on a staggered mesh: *Journal of Computational Physics*, **154**, 520–527.
- Carcione, J. M., H. B. Helle, and N. H. Pham, 2000a, White's model for wave propagation in partially saturated rocks: Comparison with poroelastic numerical experiments: *Geophysics*, **68**, 1389–1398.
- Carcione, J. M., G. Herman, and F. P. E. ten Kroode, 2002, Seismic modeling: *Geophysics*, **67**, 1304–1325.
- Carcione, J. M., S. Picotti, D. Gei, and G. Rossi, 2006, Physics and seismic modeling for monitoring CO₂ storage: *Pure and Applied Geophysics*, **163**, 175–207.
- Carcione, J. M., and G. Quiroga-Goode, 1995, Some aspects of the physics and numerical modeling of Biot compressional waves: *Journal of Computational Acoustics*, **3**, 261–280.
- Carcione, J. M., J. E. Santos, C. L. Ravazzoli, and H. B. Helle, 2003b, Wave simulation in partially frozen porous media with fractal freezing conditions: *Journal of Applied Physics*, **94**, 7839–7847.
- Carcione, J. M., and G. Seriani, 2001, Wave simulation in frozen porous media: *Journal of Computational Physics*, **170**, 676–695.
- Chaljub, E., D. Komatitsch, J.-P. Vilotte, Y. Capdeville, B. Valette, and G. Festa, 2007, Spectral-element analysis in seismology, in R.-S. Wu, V. Maupin, and R. Dmowska, eds., Advances in wave propagation in heterogeneous media: Elsevier Scientific Publ. Co., Inc., 365–419.
- Chiavassa, G., B. Lombard, and J. Piroux, 2009, Numerical modeling of 1-D transient poroelastic waves in the low-frequency range: *Journal of Computational and Applied Mathematics*, **234**, 1757–1765, doi: 10.1016/j.cam.2009.08.025.
- Claerbout, J. F., 1971, Toward a unified theory of reflector mapping: *Geophysics*, **36**, 467–481.
- Clayton, R., and B. Engquist, 1977, Absorbing boundary conditions for acoustic and elastic wave equations: *Bulletin of the Seismological Society of America*, **67**, 1529–1540.
- Dai, N., A. Vafidis, and E. Kanasewich, 1995, Wave propagation in heterogeneous porous media: A velocity-stress, finite-difference method: *Geophysics*, **60**, 327–340.
- De Barros, L., and M. Dietrich, 2008, Perturbations of the seismic reflectivity of a fluid-saturated depth-dependent poroelastic medium: *Journal of the Acoustical Society of America*, **123**, 1409–1420.
- De Basabe, J. D., and M. K. Sen, 2007, Grid dispersion and stability criteria of some common finite-element methods for acoustic and elastic wave equations: *Geophysics*, **72**, no.6, T81–T95.

- De Basabe, J. D., M. K. Sen, and M. Wheeler, 2008, The interior penalty discontinuous Galerkin method for elastic wave propagation: Grid dispersion: *Geophysical Journal International*, **175**, 83–93.
- Degrande, G., and G. De Roeck, 1992a, FFT-based spectral analysis methodology for one-dimensional wave propagation in poroelastic media: *Transport in Porous Media*, **9**, 85–97.
- , 1992b, A spectral element method for two-dimensional wave propagation in horizontally layered saturated porous media: *Computers and Structures*, **44**, 717–728.
- Degrande, G., G. De Roeck, P. Van Den Broeck, and D. Smeulders, 1998, Wave propagation in layered dry, saturated and unsaturated poroelastic media: *International Journal of Solids and Structures*, **35**, 4753–4778.
- de la Puente, J., M., Dumbser, M. Käser, and H. Igel, 2008, Discontinuous Galerkin methods for wave propagation in poroelastic media: *Geophysics*, **73**, no. 5, T77–T97.
- Diaz, J., and A. Ezziani, 2010, Analytical solution for wave propagation in heterogeneous acoustic/porous media. Part I: The 2D case: *Communications in Computational Physics*, **7**, no. 1, 171–194.
- Douglas, J. Jr., J. E. Santos, and J. L. Hensley, 1991a, Simulation of Biot waves in a cylindrically symmetric domain: *Proceedings of the 3rd International Conference on Hyperbolic Problems: Theory, Numerical Methods and Applications*, 330–350.
- Douglas, J. Jr., J. E. Santos, J. L. Hensley, and M. E. Morley, 1991b, Simulation of waves arising in acoustic well-logging: *Rendiconti del Seminario Matematico dell'Universita e del Politecnico di Torino, Special Issue*, 223–243.
- Douglas, J. Jr., J. E. Santos, D. Sheen, and L. S. Bennethum, 1993, Frequency domain treatment of one-dimensional scalar waves: *Mathematical Models and Methods in Applied Sciences*, **3**, 171–194.
- Douglas, J. Jr., J. E. Santos, D. Sheen, and X. Ye, 1999, Nonconforming Galerkin methods based on quadrilateral elements for second order elliptic problems: *Mathematical Modelling and Numerical Analysis*, **33**, 747–770.
- Doyle, J. F., 1997, *Wave propagation in structures*: Springer-Verlag New York.
- Fischer, P. F., and E. M. Rønquist, 1994, Spectral element methods for large scale parallel Navier-Stokes calculations: *Computer Methods in Applied Mechanics and Engineering*, **116**, 69–76.
- Garg, S. K., A. H. Nayfeh, and A. J. Good, 1974, Compressional waves in fluid-saturated elastic porous media: *Journal of Applied Physics*, **45**, 1968–1974.
- Göransson, P., 2006, Acoustic and vibrational damping in porous solids: *Philosophical Transactions of the Royal Society A*, **364**, 89–108.
- Gurevich, B., 1996, On: "Wave propagation in heterogeneous, porous media: A velocity-stress, finite difference method," by N. Dai, A. Vafidis, and E. R. Kanasewich (March–April 1995, *Geophysics*, pp. 327–340): *Geophysics*, **61**, 1230–1232.
- Haines, S., and S. R. Pride, 2006, Seismoelectric numerical modeling on a grid: *Geophysics*, **71**, no. 6, N57–N65.
- Hanyga, A., and J.-F. Lu, 2005, Wave field simulation for heterogeneous transversely isotropic porous media with the JKD permeability: *Computational Mechanics*, **36**, 196–208.
- Hassanzadeh, S., 1991, Acoustic modeling in fluid-saturated porous media: *Geophysics*, **56**, 424–435.
- Helle, H. B., N. H. Pham, and J. M. Carcione, 2003, Velocity and attenuation in partially saturated rocks: Poroelastic numerical experiments: *Geophysical Prospecting*, **51**, 551–566.
- Hensley, J. L., J. Douglas Jr., and J. E. Santos, 1991, Dispersion of type-II Biot waves in inhomogeneous media: *Proceedings of the 6th International Conference on Mathematical Methods in Engineering*, 67–83.
- Hörnl, H.-E., 2005, 3D hierarchical *hp*-FEM applied to elasto-acoustic modelling of layered porous media: *Journal of Sound and Vibration*, **285**, 341–363.
- Hörnl, H.-E., M. Nordström, and P. Göransson, 2001, A 3-D hierarchical FE formulation of Biot's equations for elasto-acoustic modelling of porous media: *Journal of Sound and Vibration*, **245**, 633–652.
- Hornbostel, S., and A. H. Thompson, 2007, Waveform design for electroseismic exploration: *Geophysics*, **72**, no. 2, Q1–Q10.
- Houmat, A., 1997, Hierarchical finite element analysis of the vibration of membranes: *Journal of Sound and Vibration*, **201**, 465–472.
- Igawa, H., K. Komatsu, I. Yamaguchi, and T. Kasai, 2004, Wave propagation analysis of frame structures using the spectral element method: *Journal of Sound and Vibration*, **277**, 1071–1081.
- Johnson, D. L., J. Koplik, and R. Dashen, 1987, Theory of dynamic permeability and tortuosity in fluid-saturated porous media: *Journal of Fluid Mechanics*, **176**, 379–402.
- Keehm, Y., 2003, *Computational rock physics: Transport properties in porous media and applications*: Ph.D. dissertation, Stanford University.
- Kelder, O., and D. M. J. Smeulders, 1997, Observation of the Biot slow wave in water-saturated Nivelsteiner Sandstone: *Geophysics*, **62**, 1794–1796.
- Komatitsch, D., 1997, Méthodes spectrales et éléments spectraux pour l'équation de l'élastodynamique 2D et 3D en milieu hétérogène (Spectral and spectral-element methods for the 2D and 3D elastodynamics equations in heterogeneous media): Ph.D. dissertation, Institut de Physique du Globe.
- Komatitsch, D., C. Barnes, and J. Tromp, 2000a, Simulation of anisotropic wave propagation based upon a spectral element method: *Geophysics*, **65**, 1251–1260.
- , 2000b, Wave propagation near a fluid-solid interface: A spectral element approach: *Geophysics*, **65**, 623–631.
- Komatitsch, D., J. Ritsema, and J. Tromp, 2002, The spectral-element method, Beowulf computing, and global seismology: *Science*, **298**, 1737–1742.
- Komatitsch, D., and J.-P. Vilotte, 1998, The spectral element method: An efficient tool to simulate the seismic response of 2D and 3D geological structures: *Bulletin of the Seismological Society of America*, **88**, 368–392.
- Leclaire, P., F. Cohen-Tenoudji, and J. Aguirre Puente, 1994, Extension of Biot's theory to wave propagation in frozen porous media: *Journal of the Acoustical Society of America*, **96**, 3753–3767.
- Liu, Q., and J. Tromp, 2008, Finite-frequency sensitivity kernels for global seismic wave propagation based upon adjoint methods: *Geophysical Journal International*, **174**, 265–286.
- Liu, X., S. Greenhalgh, and B. Zhou, 2009, Transient solution for poro-viscoacoustic wave propagation in double porosity media and its limitations: *Geophysical Journal International*, **178**, 375–393.
- Lovera, O. M., and J. E. Santos, 1988, Numerical methods for a model for wave propagation in composite anisotropic media: *Modélisation Mathématique et Analyse Numérique*, **22**, 159–176.
- Lu, J.-F., and A. Hanyga, 2004, Numerical modeling method for wave propagation in a linear viscoelastic medium with singular memory: *Geophysical Journal International*, **159**, 688–702.
- Luo, Y., H. Zhu, T. Nissen-Meyer, C. Morency, and J. Tromp, 2009, Seismic modeling and imaging based upon spectral-element and adjoint methods: *The Leading Edge*, **28**, 568–574.
- Maday, Y., and E. M. Rønquist, 1990, Optimal error analysis of spectral methods with emphasis on non-constant coefficients and deformed geometries: *Computer Methods in Applied Mechanics and Engineering*, **80**, 91–115.
- Martin, R., D. Komatitsch, and A. Ezziani, 2008, An unsplit convolutional perfectly matched layer improved at grazing incidence for seismic wave propagation in poroelastic media: *Geophysics*, **73**, no. 4, T51–T61.
- Masson, Y. J., and S. R. Pride, 2007, Poroelastic finite difference modeling of seismic attenuation and dispersion due to mesoscopic-scale heterogeneity: *Journal of Geophysical Research*, **112**, B03204.
- , 2010, Finite-difference modeling of Biot's poroelastic equations across all frequencies: *Geophysics*, **75**, no. 2, N33–N41.
- Masson, Y. J., S. R. Pride, and K. T. Nihei, 2006, Finite difference modeling of Biot's poroelastic equations at seismic frequencies: *Journal of Geophysical Research*, **111**, B10305.
- Mikhailenko, B. G., 1985, Numerical experiment in seismic investigations: *Journal of Geophysics*, **58**, 101–124.
- Mikhailov, O. V., M. W. Haartsen, and M. N. Töksoz, 1997, Electroseismic investigation of the shallow subsurface: Field measurements and numerical modeling: *Geophysics*, **62**, 97–105.
- Morency, C., Y. Luo, and J. Tromp, 2009, Finite-frequency kernels for wave propagation in porous media based upon adjoint methods: *Geophysical Journal International*, **179**, 1148–1168.
- Morency, C., and J. Tromp, 2008, Spectral-element simulations of wave propagation in porous media: *Geophysical Journal International*, **175**, 301–345.
- Müller, T., B. Gurevich, and M. Lebedev, 2010, Seismic wave attenuation and dispersion due to wave-induced flow at mesoscopic heterogeneities — A review: *Geophysics*, **75**, no. 5.
- Nedelec, J. C., 1980, Mixed finite elements in \mathbf{R}^3 : *Numerical Mathematics*, **35**, 315–341.
- Özdenvar, T., and G. McMechan, 1997, Algorithms for staggered-grid computations for poroelastic, elastic, acoustic, and scalar wave equations: *Geophysical Prospecting*, **45**, 403–420.
- Patera, A. T., 1984, A spectral element method for fluid dynamics: Laminar flow in a channel expansion: *Journal of Computational Physics*, **54**, 468–488.
- Picotti, S., J. M. Carcione, J. G. Rubino, and J. E. Santos, 2007, P-wave seismic attenuation by slow-wave diffusion: Numerical experiments in partially saturated rocks: *Geophysics*, **72**, no. 4, N11–N21.
- Pride, S. R., 1994, Governing equations for the coupled electromagnetics and acoustics of porous media: *Physics Review B*, **50**, 15678–15696.
- Pride, S. R., J. G. Berryman, and J. M. Harris, 2004, Seismic attenuation due to wave-induced flow: *Journal of Geophysical Research*, **109**, B01201.1–B01201.19.
- Pride, S. R., and M. W. Haartsen, 1996, Electroseismic wave properties: *Journal of the Acoustical Society of America*, **100**, 1301–1315.
- Quiroga-Goode, G., S. Jiménez-Hernández, M. A. Pérez-Flores, and R. Padilla-Hernández, 2005, Computational study of seismic waves in homogeneous dynamic-porosity media with thermal and fluid relaxation: Gauging

- Biot theory: *Journal of Geophysical Research*, **110**, B07303.
- Ravazzoli, C. L., and J. E. Santos, 2005, A theory for wave propagation in porous rocks saturated by two-phase fluids under variable pressure conditions: *Bollettino di Geofisica Teorica ed Applicata*, **46**, 261–285.
- Ravazzoli, C. L., J. E. Santos, and J. M. Carcione, 2003, Acoustic and mechanical response of reservoir rocks under variable saturation and effective pressure: *Journal of the Acoustical Society of America*, **113**, 1801–1811.
- Raviart, P. A., and J. M. Thomas, 1977, A mixed finite element method for second order elliptic problems: *Proceedings of the Mathematical Aspects of Finite Element Methods Conference*, 292–315.
- Rizzi, S. A., and J. F. Doyle, 1992, A spectral element approach to wave motion in layered solids: *Journal of Vibration and Acoustics*, **114**, 569–577.
- Rosenbaum, J. H., 1974, Synthetic microseismograms: Logging in porous formations: *Geophysics*, **39**, 14–32.
- Rubino, J. G., C. L. Ravazzoli, and J. E. Santos, 2006a, Reflection and transmission of waves in composite porous media: A quantification of slow waves conversions: *Journal of the Acoustical Society of America*, **120**, 2425–2436.
- , 2008, Biot-type scattering effects in gas-hydrate bearing sediments: *Journal of Geophysical Research*, **113**, B06102.
- , 2009, Equivalent viscoelastic solids for heterogeneous fluid-saturated porous rocks: *Geophysics*, **74**, no. 1, N1–N13.
- Rubino, J. G., J. E. Santos, S. Picotti, and J. M. Carcione, 2006b, Simulation of upscaling effects due to wave-induced fluid flow in Biot media using the finite-element method: *Journal of Applied Geophysics*, **62**, 193–203.
- Saenger, E. H., R. Ciz, O. S. Krüger, S. M. Schmalholz, B. Gurevich, and S. A. Shapiro, 2007, Finite-difference modeling of wave propagation on microscale: A snapshot of the work in progress: *Geophysics*, **72**, no. 5, SM293–SM300.
- Sanchez Palencia, E., 1980, *Non-homogeneous media and vibration theory*: Springer-Verlag New York, Inc.
- Santos, J. E., 1986, Elastic wave propagation in fluid-saturated porous media, Part I: The existence and uniqueness theorems: *Mathematical Modelling and Numerical Analysis*, **20**, 113–128.
- , 2009, Finite element approximation of coupled seismic and electromagnetic waves in fluid-saturated poroviscoelastic media: *Numerical Methods for Partial Differential Equations*, doi: 10.1002/num.20527.
- Santos, J. E., J. M. Corbero, and J. Douglas Jr., 1990a, Static and dynamic behavior of a porous solid saturated by a two-phase fluid: *Journal of the Acoustical Society of America*, **87**, 1428–1438.
- Santos, J. E., J. Douglas Jr., and A. P. Calderón, 1988a, Finite element methods for a composite model in elastodynamics: *SIAM Journal of Numerical Analysis*, **25**, 513–532.
- Santos, J. E., J. Douglas Jr., J. M. Corbero, and O. M. Lovera, 1990b, A model for wave propagation in a porous medium saturated by a two-phase fluid: *Journal of the Acoustical Society of America*, **87**, 1439–1448.
- Santos, J. E., J. Douglas Jr., M. E. Morley, and O. M. Lovera, 1988b, Finite element methods for a model for full waveform acoustic logging: *Institute for Mathematics and Applications Journal of Numerical Analysis*, **8**, 415–433.
- Santos, J. E., and E. J. Oreña, 1986, Elastic wave propagation in fluid-saturated porous media, Part II: The Galerkin procedures: *Mathematical Modelling and Numerical Analysis*, **20**, 129–139.
- Santos, J. E., C. L. Ravazzoli, and J. M. Carcione, 2004a, A model for wave propagation in a composite solid matrix saturated by a single-phase fluid: *Journal of the Acoustical Society of America*, **115**, 2749–2760.
- Santos, J. E., C. L. Ravazzoli, J. M. Carcione, P. M. Gauzellino, and F. Cavallini, 2002, Prediction and simulation of a second slow wave in partially saturated porous media: 64th Conference & Technical Exhibition, EAGE, Extended Abstracts, 261–285.
- Santos, J. E., C. L. Ravazzoli, P. M. Gauzellino, J. M. Carcione, and F. Cavallini, 2004b, Simulation of waves in poro-viscoelastic rocks saturated by immiscible fluids — Numerical evidence of a second slow wave: *Journal of Computational Acoustics*, **12**, 1–21.
- Santos, J. E., C. L. Ravazzoli, and J. Geiser, 2005, On the static and dynamic behavior of fluid saturated composite porous solids: A homogenization approach: *International Journal of Solids and Structures*, **43**, 1224–1238.
- Santos, J. E., J. G. Rubino, and C. L. Ravazzoli, 2009, A numerical upscaling procedure to estimate effective plane wave and shear moduli in heterogeneous fluid-saturated poroelastic media: *Computer Methods in Applied Mechanics and Engineering*, **198**, 2067–2077.
- Santos, J. E., and D. Sheen, 2007, Finite element methods for the simulation of waves in composite saturated poroviscoelastic materials: *SIAM Journal of Numerical Analysis*, **45**, 389–420.
- , 2008, Derivation of a Darcy's law for composite porous solids using a homogenization technique: *Transport in Porous Media*, **74**, 349–368.
- Seriani, G., E. Priolo, J. M. Carcione, and E. Padovani, 1992, High-order spectral element method for elastic wave modeling: 62nd Annual International Meeting, SEG, Expanded Abstracts, 1285–1288.
- Stern, M., A. Bedford, and H. R. Millwater, 1985, Wave reflection from a sediment layer with depth-dependent properties: *Journal of the Acoustical Society of America*, **77**, 1781–1788.
- Tarantola, A., 1984, Inversion of seismic reflection data in the acoustic approximation: *Geophysics*, **49**, 1259–1266.
- , 1987, Inverse problem theory: Methods for data fitting and model parameter estimation: Elsevier Scientific Publ. Co., Inc.
- Teng, Y.-C., 1990, Finite element results of the slow compressional wave in a porous medium at ultrasonic frequencies: *Journal of Applied Physics*, **68**, 4335–4337.
- Thompson, A. H., 2005, Electromagnetic-to-seismic conversion: Successful developments suggest viable applications in exploration and production: 75th Annual International Meeting, SEG, Expanded Abstracts, 554–558.
- Thompson, A. H., and G. Gist, 1993, Geophysical applications of electrokinetic conversion: *The Leading Edge*, **12**, 1169–1163.
- Tromp, J., C. H. Tape, and Q. Liu, 2005, Seismic tomography, adjoint methods, time reversal, and banana-doughnut kernels: *Geophysical Journal International*, **160**, 195–216.
- Turgut, A., and T. Yamamoto, 1988, Synthetic seismograms for marine sediments and determination of porosity and permeability: *Geophysics*, **53**, 1056–1067.
- Vasco, D. W., 2008, Modelling quasi-static poroelastic propagation using an asymptotic approach: *Geophysical Journal International*, **173**, 1119–1135.
- Wenzlau, F., and T. M. Müller, 2009, Finite-difference modeling of wave propagation and diffusion in poroelastic media: *Geophysics*, **74**, no. 4, T55–T66.
- Wheeler, M., 1978, An elliptic collocation-finite element method with interior penalties: *SIAM Journal of Numerical Analysis*, **15**, 152–161.
- White, J. E., 1975, Computed seismic speeds and attenuation in rocks with partial gas saturation: *Geophysics*, **40**, 224–232.
- Zeng, Y. Q., J. Q. He, and Q. H. Liu, 2001, The application of the perfectly matched layer in numerical modeling of wave propagation in poroelastic media: *Geophysics*, **66**, 1258–1266.
- Zhang, J., 1999, Quadrangle-grid velocity-stress finite difference method for poroelastic wave equations: *Geophysical Journal International*, **139**, 171–182.
- Zhang, J., and H. Gao, 2009, Elastic wave modelling in 3-D fractured media: An explicit approach: *Geophysical Journal International*, **177**, 1233–1241.
- Zhu, H., Y. Luo, T. Nissen-Meyer, C. Morency, and J. Tromp, 2009, Elastic imaging and time-lapse migration based upon adjoint methods: *Geophysics*, **74**, no. 6, WCA167–WCA177.
- Zhu, X., and G. A. McMechan, 1991, Numerical simulation of seismic responses of poroelastic reservoirs using Biot theory: *Geophysics*, **56**, 328–339.
- Zyserman, F. I., P. M. Gauzellino, and J. E. Santos, 2003, Dispersion analysis of a nonconforming finite element method for the Helmholtz and elastodynamic equations: *International Journal for Numerical Methods in Engineering*, **58**, 1381–1395.
- Zyserman, F. I., P. M. Gauzellino, and J. E. Santos, 2010, Finite element modeling of SHTE and PVSTM electroseismics: *Journal of Applied Geophysics*, doi: 10.1016/j.jappgeo.2010.07.004.
- Zyserman, F. I., and J. E. Santos, 2007, Analysis of the numerical dispersion of waves in saturated poroelastic media: *Computer Methods in Applied Mechanics and Engineering*, **196**, 4644–4655.